



Published in final edited form as:

*Cancer Lett.* 2021 October 28; 519: 304–314. doi:10.1016/j.canlet.2021.07.040.

## PCNA Inhibition Enhances the Cytotoxicity of $\beta$ -Lapachone in NQO1-Positive Cancer Cells by Augmentation of Oxidative Stress-induced DNA Damage

Xiaolin Su<sup>#a</sup>, Jiangwei Wang<sup>#b</sup>, Lingxiang Jiang<sup>b</sup>, Yaomin Chen<sup>c</sup>, Tao Lu<sup>d</sup>, Marc S Mendonca<sup>b</sup>, Xiumei Huang<sup>b,#</sup>

<sup>a</sup>Department of Biochemistry and Molecular Biology, Indiana University Melvin and Bren Simon Comprehensive Cancer Center, Indiana University School of Medicine, Indianapolis, IN 46202, USA

<sup>b</sup>Department of Radiation Oncology, Indiana University Melvin and Bren Simon Comprehensive Cancer Center, Indiana University School of Medicine, Indianapolis, IN 46202, USA

<sup>c</sup>Indiana University Health Pathology Laboratory, Indiana University School of Medicine, Indianapolis, Indiana 46202 USA

<sup>d</sup>Department of Pharmacology and Toxicology, Indiana University Melvin and Bren Simon Comprehensive Cancer Center, Indiana University School of Medicine, Indianapolis, IN 46202, USA

# These authors contributed equally to this work.

### Abstract

$\beta$ -Lapachone is a classic quinone-containing antitumor NQO1-bioactivatable drug that directly kills NQO1-overexpressing cancer cells. However, the clinical applications of  $\beta$ -lapachone are primarily limited by its high toxicity and modest lethality. To overcome this side effect and expand the therapeutic utility of  $\beta$ -lapachone, we demonstrate the effects of a novel combination therapy including  $\beta$ -lapachone and the proliferating cell nuclear antigen (PCNA) inhibitor T2 amino alcohol (T2AA) on various *NQO1*<sup>+</sup> cancer cells. PCNA has DNA clamp processivity activity mediated by encircling double-stranded DNA to recruit proteins involved in DNA replication and DNA repair. In this study, we found that compared to monotherapy, a nontoxic dose of the

---

# **Corresponding Author:** Xiumei Huang, Indiana University School of Medicine, 980 West Walnut Street, R3, C511, Indianapolis, IN 46202. xiuhuang@iu.edu.

Author contributions

J. Wang, X. Su and X. Huang designed the experiments, analyzed the data, and wrote the manuscript. X. Huang supervised the project. J. Wang, X. Su, L. Jiang, Y. Chen, T. Lu, MS. Mendonca and X. Huang reviewed and edited the manuscript.

Declarations of interest

There are no potential conflicts of interest to disclose.

Declaration of interests

The authors declare that they have no known competing financial interests or personal relationships that could have appeared to influence the work reported in this paper.

**Publisher's Disclaimer:** This is a PDF file of an unedited manuscript that has been accepted for publication. As a service to our customers we are providing this early version of the manuscript. The manuscript will undergo copyediting, typesetting, and review of the resulting proof before it is published in its final form. Please note that during the production process errors may be discovered which could affect the content, and all legal disclaimers that apply to the journal pertain.

T2AA synergized with a sublethal dose of  $\beta$ -lapachone in an NQO1-dependent manner and that combination therapy prevented DNA repair, increased double-strand break (DSB) formation and PARP1 hyperactivation and induced catastrophic energy loss. We further determined that T2AA promoted programmed necrosis and G1/S phase cell cycle arrest in  $\beta$ -lapachone-treated *NQO1*<sup>+</sup> cancer cells. Our findings show novel evidence for a new therapeutic approach that combines of  $\beta$ -lapachone treatment with PCNA inhibition that is highly effective in treating *NQO1*<sup>+</sup> solid tumor cells.

## Keywords

NQO1;  $\beta$ -Lapachone; PCNA; T2AA; combination chemotherapy

## 1. Introduction

Cancer is a common disease that despite treatment advances remains the second leading cause of death worldwide which is only exceeded by cardiovascular disease [1, 2]. In 2020, more than 1.8 million new cancer cases and 0.6 million cancer deaths were projected to occur in the United States, as reported by the U.S. Centers for Disease Control and Prevention [3]. Targeted therapy is a therapeutic approach that seeks to accurately identify the genetic and biochemical changes in various cancer types and then chemically or biologically target these alterations to specifically kill these cancer cells [4, 5]. NAD(P)H:quinone oxidoreductase-1 (NQO1) is considered to be one of these cancer-specific targets. NQO1 is overexpressed in most solid cancers (e.g., non-small cell lung, pancreatic, breast, prostate, colon and head and neck), with very low expression in normal cells/tissue [6–10].  $\beta$ -Lapachone ( $\beta$ -lap, ARQ761 in clinical form) is a classic natural naphthoquinone compound that was originally derived from the bark of the lapacho tree in Central and South America in the 1960s with potential antineoplastic activity, it is bioactivated by the flavo-enzyme NQO1 [11, 12]. It has a wide range of activities, including antiviral, antifungal, antibacterial and antitumor properties.  $\beta$ -Lap has been shown to be a highly specific, stable and effective antitumor agent, and has been confirmed as a first-generation NQO1-bioactivatable drug [13, 14].

Over the last 30 years the mechanism of  $\beta$ -lap antitumor activity has been elucidated and shown to involve the induction of a futile NQO1-dependent redox cycle, where the drug forms an unstable hydroquinone that spontaneously oxidizes back to the parent compound in a two-step oxygenation process [15, 16]. This futile redox cycle results in continual oxygen consumption that leads to massive reactive oxygen species (ROS) generation and calcium release from endoplasmic reticulum (ER) stores [17]. These cell membrane-permeable ROS have been shown to diffuse into the cell nucleus and induce extensive DNA lesions including DNA base damage and single and double DNA strand breaks. This DNA damage triggers DNA repair mechanisms such as single-strand break repair (SSBR), homologous recombination (HR), nonhomologous end joining (NHEJ) and base excision repair (BER) [18].  $\beta$ -Lap induced-ROS can induce PARP-1 hyperactivation at the time of DNA lesion accumulation that exceeds the functional DNA repair machinery competence [19, 20]. This series of processes facilitates the formation and degradation of the DNA repair protein

PARylation (PAR), and in the severe depletion of NAD<sup>+</sup>/ATP nucleotide levels [21]. NQO1 overexpressing tumor cells are particularly sensitive to this ROS induction and NAD<sup>+</sup>/ATP depletion induced by  $\beta$ -lap and which results in NQO1 overexpressing tumor cells to undergo  $\mu$ -calpain-mediated caspase-independent programmed necrosis [22]. Therefore,  $\beta$ -lap and its derivatives have been developed as potential promising targeted antitumor drug candidates for a wide range of tumor types to over the last few years [23, 24].

Proliferating cell nuclear antigen (PCNA), a homotrimeric protein complex, plays an essential role as a processivity-promoting factor that orchestrates and organizes many aspects of key DNA replication and DNA repair processes [25, 26]. First, PCNA, as a DNA clamp, needs to load the circular DNA clamp loader replication factor C (RFC) in an ATP-dependent manner [27]. With the help of RFC, PCNA encircles double-stranded DNA in addition to sliding spontaneously across it [28]. Once bound to DNA, the complex serves as a binding platform for recruiting and coordinating multiple regulatory DNA replication and DNA repair proteins linked to DNA metabolic pathways [29, 30]. The small-molecule PCNA inhibitor T2 amino alcohol (T2AA), a T3 derivative that exhibits little thyroid hormone activity, inhibits PCNA functions. The crystal structure of the two-molecule T2AA complex with one molecule of PCNA demonstrates that T2AA is bound to the surface adjacent to the subunit interface of PCNA and also to the PIP-box binding site that inhibits the interaction of PCNA/PIP-box peptide [31, 32].

Although  $\beta$ -lap is a reliable and validated antitumor agent *in vitro*, to date *in vivo* translation has encountered some limitations and hurdles [9]. A large amount of experimental laboratory data shows that while  $\beta$ -lap leads to modest tumor-selective lethality *in vitro* it also triggers acute toxicity *in vivo* [33]. Mice exhibit severe labored breathing, muscle contractions and even immediate death in some cases after  $\beta$ -lap dosing [34]. All of the above factors have severely hindered further clinical exploitation and utilization of  $\beta$ -lap. We proposed that the antitumor effect of  $\beta$ -lap is closely bound to DNA damage and repair processes, and that blocking PCNA activity with T2AA treatment will further inhibit DNA repair enhance tumor cytotoxicity [35]. We show here that the combination of low dose  $\beta$ -lap with T2AA generates synergistic antitumor effects in non-small cell lung, breast and pancreatic cancers.

## 2. Materials and Methods

### 2.1. Cell lines and culture

Human non-small cell lung cancer (NSCLC) cells were a generous gift from UTSW-MD Anderson SPORE in Lung Cancer. The human pancreatic adenocarcinoma (PDA) cancer cell lines MiaPaCa2 and BxPC-3 and the human breast cancer cell lines MCF-7 and MDA-MB-231 were originally obtained from the American Tissue Culture Collection (ATCC). A549 and MDA-MB-231 NQO1-deficient and NQO1-proficient cell lines were generated as previously described [7]. All cell lines were cultured in Dulbecco's modified Eagle's medium (DMEM) or RPMI medium supplemented with 10% fetal bovine serum (FBS). Cells were incubated at 37°C in a humidified 5% CO<sub>2</sub>-95% air atmosphere and routinely screened to demonstrate that they were free of mycoplasma contamination.

## 2.2. Antibodies

The antibodies used for immunofluorescence and western blotting included anti-NQO1 (1:200, sc-32793, Santa Cruz Biotechnology), anti-PARP1 (1:500, 4338-MC-50, Trevigen), anti- $\beta$ -actin (1:1000, sc-47778, Santa Cruz Biotechnology), anti-PAR (1:200, sc-56198, Santa Cruz Biotechnology), anti-cleaved caspase-3 (1:500, 9661S, Cell Signaling Technology), anti-cleaved caspase-7 (1:500, 9491S, Cell Signaling Technology), anti-PCNA (1:1000, 25865, Cell Signaling Technology), anti- $\gamma$ -H2AX (1:1000, JBW301, Millipore), anti- $\alpha$ -tubulin (1:1000, Santa Cruz Biotechnology), anti-P53 (1:200, DO-1, Santa Cruz Biotechnology), and anti-53BP1 (1:1000, NB 100–304, Novus Biologicals).

## 2.3. Reagents and chemicals

$\beta$ -Lap (3,4-dihydro-2,2-dimethyl-2H-naphtho[1,2-b]pyran-5,6-dione) was synthesized and purified in our laboratory, confirmed by NMR, and dissolved in dimethyl sulfoxide (DMSO) at 48 mM, concentrations were verified by spectrophotometry. Other reagents and chemicals were obtained from Sigma-Aldrich and included (S)-4-(4-(2-amino-3-hydroxypropyl)-2,6-diiodophenoxy) phenol hydrochloride (T2AA, SML 0794), dicoumarol (DIC, 287897), hydrogen peroxide (H<sub>2</sub>O<sub>2</sub>, HX0636), and 2',7'-dichlorofluorescein diacetate (DCFDA, 35845).

## 2.4. Relative survival assays (DNA assay)

A relative survival assay was performed as previously described [36]. Briefly, cells were seeded at  $1 \times 10^4$  per well in 48-well plates and allowed to attach overnight. The cells were pretreated with T2AA (20  $\mu$ M, 2 h) or left untreated and then cotreated with various doses of  $\beta$ -lap (2 h) as indicated in the presence or absence of 50  $\mu$ M DIC. Then, drug-free medium was added, and the cells were grown for 5 to 7 days until the control cells reached ~90% confluence. The medium was removed, and the cells were washed with  $1 \times$  PBS. The PBS was discarded, and 250  $\mu$ L of ddH<sub>2</sub>O was added to each well. The cells were lysed by a freeze-thaw method and stained with 500  $\mu$ L of Hoechst dye (from a stock of 50  $\mu$ L of Hoechst 33258 (Sigma-Aldrich, 14530) in 50 mL of  $1 \times$  TNE buffer) and incubated in the dark for 2 h at room temperature. DNA content was quantified by fluorescence (460 nm) in a Victor X3 Plate reader (Perkin-Elmer, Waltham, MA). Data are expressed as the treated/control (T/C) ratio from at least triplicate experiments (mean  $\pm$  SD). Statistical analyses methods for all endpoints are described below.

## 2.5. O<sub>2</sub> consumption rate (OCR) assessment

OCR assessments were performed using a Seahorse XF96 analyzer (Agilent Technologies) as described previously [16]. Cells were plated at a seeding density of 30000/well in Seahorse XF96 cell culture microplates and grown overnight. The following day, real-time OCR measurements were monitored using the machine and Seahorse medium containing exclusively glucose and glutamine, according to the manufacturer's instructions. Data were analyzed on a Seahorse XF bioanalyzer for 2 h. The results are graphed as the mean  $\pm$  SD from at least three independent experiments for each treatment group and were determined.

## 2.6. ROS measurement

The detailed protocol for ROS detection and quantification has been described previously [37]. In brief, cells were plated in 6-well plates at 70% confluence and allowed to attach overnight. The following day, the cells were treated with appropriate drug treatments, followed by treatment with 10  $\mu$ M DCFDA and incubation for 30 min at 37°C. Then, the cells were trypsinized and centrifuged for 5 min at 15000 x rpm and resuspended in 200–500  $\mu$ L of ice-cold PBS. Green cell fluorescence was determined by flow cytometry (FCM) using a flow cytometer (BD Biosciences) and FlowJo acquisition software. The mean  $\pm$  SD ROS levels from three independent experiments for each treatment group were determined.

## 2.7. Western blotting

Total protein was extracted from cells, and the protein concentrations of all extractions were measured using the Bio-Rad protein assay in conjunction with bovine serum albumin standards. Protein samples were fractionated by 7.5%~12% SDS-PAGE and then transferred to PVDF membranes [38]. After antibody incubation, western blotting was performed using enhanced chemiluminescent detection (SuperSignal West Dura, Fisher 34076), and the band intensity in each group was measured with NIH ImageJ software and normalized to that of the internal control [39].

## 2.8. H<sub>2</sub>O<sub>2</sub>, ATP and NAD<sup>+</sup> quantification

H<sub>2</sub>O<sub>2</sub> (ROS-Glo), ATP (CellTiter-Glo) and NAD/NADH (NAD/NADH-Glo) were assayed at the indicated time points during or after treatments using standard chemical assays following manufactures' protocols. (Promega G8820, Promega G9071, Promega G7572).

## 2.9. PCNA knockdown by siRNA

PCNA-specific siRNA (CCUUGGCGCUAGUAUUUGAtt, GAGUACAGCUGUGUAGUAAAtt, GUACCUGAACUUCUUUACAtt, 20 nM, Santa Cruz sc-29440. ) or a scrambled siRNA control (20 nM, Thermo Scientific D-001210-01-20) was transiently transfected into cells using Opti-MEM and Lipofectamine RNAiMAX (Life Technologies) according to the manufacturer's instructions. Forty-eight hours after transfection, the cells were collected for subsequent experiments. Knockdown of PCNA protein levels were confirmed by Western blotting [40].

## 2.10. Immunofluorescence assay

Cells were imaged using a Leica DM5500 fluorescence microscope to evaluate two markers of double-strand break (DSB) formation 53BP1 and  $\gamma$ -H2AX foci detected by immunofluorescence. The mean  $\pm$  SD number of 53BP1 and  $\gamma$ -H2AX foci in 50 to 100 cell nuclei were quantified and graphed for each treatment group [9]. The mean  $\pm$  SD foci number from three independent experiments for each treatment group versus time were determined.

## 2.11. Alkaline comet assay

Alkaline comet assays (Cell Biolabs STA-355) were performed to measure total DNA lesions, including DNA bases, single-strand breaks (SSBs), and DSBs, were assessed using

single-cell gel electrophoresis. Slides were stained with SYBR green and visualized by using a Leica DM5500 microscope. Comet tail lengths were quantified by NIH ImageJ software. Each data point was calculated as an average of 100 cells, and samples were performed in triplicate for each treatment group.

### 2.12. Cell cycle assay

Cells were harvested for controls and each treatment group by trypsin treatment and fixed overnight with 100% (v/v) ethanol at  $-20^{\circ}\text{C}$ . The cells were then centrifuged, the supernatant was removed, and the cells were washed with PBS, suspended in cold PBS, and passed through a 27-G needle until a homogenous cell suspension was obtained. Then, the cells were resuspended in saponin-based permeabilization buffer, incubated for 30 min in a  $37^{\circ}\text{C}$  TC incubator and resuspended in  $1\times$  Click-iT cell reaction buffer in a  $38^{\circ}\text{C}$  TC incubator for 2–3 h. Finally, the cells were resuspended in a propidium iodide (PI) and 5-ethynyl-2'-deoxyuridine (EdU) solution. The final results were analyzed by flow cytometry using a flow cytometer (BD Biosciences) and FlowJo acquisition software [9].

### 2.13. In vivo antitumor studies

The *in vivo* xenograft model was generated by injecting  $2\times 10^6$  Lewis lung carcinoma (LLC) cells into the subcutaneous space on the right flank of C57BL/6 female mice weighing  $\sim 20\text{g}$  obtained from the Jackson Laboratory. Tumor volumes were measured with a caliper and calculated by the formula  $0.5\times \text{length}\times \text{width}^2$ . When tumor volume reached  $\sim 50\text{--}80\text{ mm}^3$ , mice were randomly divided into four groups with no statistical differences in tumor sizes. Mice were then treated with HP $\beta$ CD, T2AA (20 mg/kg), HP $\beta$ CD- $\beta$ -lap (18 mg/kg) or T2AA (20 mg/kg) plus HP $\beta$ CD- $\beta$ -lap (18 mg/kg) by intra-tumor injection once per day for five consecutive days. Two days later, another five treatments were repeated. When tumor volume reached  $\sim 2000\text{ mm}^3$ , mice were sacrificed and survival curve was plotted. All animal studies were carried out under the Indiana University School of Medicine Institutional Animal Care and Use Committee (IACUC)-approved protocol and in accordance with the guidelines for ethical conduct in the care and use of animals in research.

### 2.14. Statistical analysis

Data (mean  $\pm$  SD) were graphed, and ANOVA was used to compare groups. Two-tailed Student's *t* tests were used for independent measures with the Holm-Sidak correction for multiple comparisons if  $>1$  comparison was performed. The minimum replicate size for any experiment was  $n = 3$ . Alpha was set to 0.05. All statistical analyses were performed with GraphPad Prism 8. Images are representative of the results of experiments or staining repeated three times. \* $p < 0.05$ , \*\* $p < 0.01$  and \*\*\* $p < 0.001$ .

### 2.15. Synergy calculations

Synergy interactions between  $\beta$ -lap and T2AA were evaluated as previously described using two methods: 1) direct comparisons made between the effect of combined treatments and the effect of individual drugs in each experiment and 2) formal synergy effect evaluations using the strict method proposed by Chou and coworkers, and pooled dose-response curves for each of the treatments were required [41].

### 3. Results

#### 3.1. The PCNA inhibitor T2AA synergizes with a sublethal dose of $\beta$ -lap in an NQO1-dependent manner

The standard approach used to evaluate the antitumor efficacy of  $\beta$ -lap has mainly relied on direct *NQO1*<sup>+</sup> cell killing assays [16]. In this investigation, we tested the hypothesis that treatment with  $\beta$ -lap and simultaneous inhibition of PCNA will inhibit DNA replication and DNA repair, leading to a synergistic effect between PCNA inhibition and  $\beta$ -lap treatment in *NQO1*<sup>+</sup> human cancer. We first tested for evidence of synergism between  $\beta$ -lap and the PCNA inhibitor T2AA in MCF-7 breast and BxPC-3 pancreatic cancer (PDAC) cells, which have high endogenous NQO1 expression (Fig. 1A,B). MCF-7 and BxPC-3 cells were pretreated with a nontoxic dose of T2AA (20  $\mu$ M) for 2 h, followed by cotreatment with doses of from 1 to 4  $\mu$ M of  $\beta$ -lap + T2AA (20  $\mu$ M) for an additional 2 h (Fig. 1A,B). The drugs were removed, and the cells were assessed for survival. T2AA dramatically increased the sensitivity of MCF-7 and BxPC-3 cells to sublethal doses at 1  $\mu$ M of  $\beta$ -lap in MCF-7 cells and at 1, 1.5, and 2  $\mu$ M in BxPC-3 cells (Fig. 1A, B). We then examined the effect of combined treatment with T2AA and  $\beta$ -lap on MiaPaCa2 pancreatic, A549 NSC lung and MDA-MB-231 breast cancer cells with knocked out or reconstituted NQO1 expression (Fig. 1C–H). MiaPaCa2 PDAC and A549 NSCLC cells expressed high NQO1 levels and were hypersensitive to the combined T2AA + nontoxic concentrations of  $\beta$ -lap (Fig. 1C, E). CRISPR/Cas9-mediated *NQO1* knockout in A549 NSCLC and MiaPaCa2 PDAC cells rendered the cells significantly resistant to the drug alone and combination treatment (Fig. 1D, F). MDA-MB-231 breast cancer cells that lack NQO1 expression due to a \*2 polymorphism were inherently resistant to combined 20  $\mu$ M T2AA and 1 to 4  $\mu$ M  $\beta$ -lap treatment (Fig. 1G), and reconstitution of *NQO1* in MDA-MB-231 cells by exogenous over-expression of NQO1 resulted in the appearance of toxicity with combined  $\beta$ -lap and T2AA treatment (Fig. 1H). Nontoxic PCNA inhibitor T2AA doses were screened for all of the above cell lines in advance and these data are presented in supplemental (Fig. S1A–H). Knockout or reconstitution of *NQO1* in MiaPaCa2, A549, and MDA-MB-231 cancer cells and the endogenous NQO1 in MCF-7 and BxPC-3 cancer cells were confirmed by western blot analysis (Fig. 1D, F, H and Fig. S1I). The Half-maximal inhibitory concentration (IC<sub>50</sub>) values of  $\beta$ -lap or T2AA for each cell line mentioned above were determined by DNA assay (Fig. S1J). Together, these findings suggest that the PCNA inhibitor T2AA enhances  $\beta$ -lap lethality in an NQO1-dependent manner.

#### 3.2. Combination therapy induces NQO1-dependent PARP1 hyperactivation, ROS formation and NAD<sup>+</sup>/ATP loss

Exposure of MiaPaCa2 PDAC cells to 1, 1.5, and 2  $\mu$ M  $\beta$ -lap for 2 h alone was relatively nontoxic (>70% survival), whereas treatment with 2.5, 3, and 4  $\mu$ M of  $\beta$ -lap was a toxic with survival < 10% (Fig. 1C). A relative cell survival assay indicated that a nontoxic dose of T2AA (20  $\mu$ M, 4 h) led to synergistic lethality with a 2 h treatment of 1, 1.5 and 2  $\mu$ M  $\beta$ -lap (Fig. 1C). In Figure 2A Oxygen Consumption Rates (OCRs) monitored by seahorse analysis indicated that treatment of MiaPaCa2 cells with 2, 4, and 8  $\mu$ M  $\beta$ -lap increased oxygen consumption with increasing dose of  $\beta$ -lap, which we have previously shown to be indicative of cells undergoing an NQO1-dependent futile redox cycle [9]. These increases in

OCR are particularly evident at the highly toxic 4 and 8  $\mu\text{M}$   $\beta$ -lap treatments. The results showed that a nontoxic dose of T2AA (20  $\mu\text{M}$ , 4 h) alone hardly increased OCRs, however, the combination of T2AA with or without a sublethal dose of  $\beta$ -lap (2 or 4  $\mu\text{M}$ , 2 h) resulted in equivalent OCRs. Interestingly, at the 8  $\mu\text{M}$   $\beta$ -lap dose, the NQO1 futile redox appears to become exhausted with a decay in OCR from its maximum of > 300 pmol/min 30 to 60 minutes after treatment to less than 150 pmol/min at the 140 minute treatment timepoint (Fig. 2A). However, this decay was not observed when the cells were treated with the combination of 8  $\mu\text{M}$   $\beta$ -lap and 20  $\mu\text{M}$  T2AA with increasing OCR to 250 pmol/min at 20 minutes and remaining elevated (Fig. 2A), suggesting that the dramatic decay in OCRs observed with 8  $\mu\text{M}$   $\beta$ -lap treatment could partially be inhibited through suppression of PCNA function by T2AA treatment.

We next examined whether T2AA affects  $\beta$ -lap-mediated induction of reactive oxygen species (ROS) formation. NQO1-related  $\text{H}_2\text{O}_2$  levels were measured in the first 2 h of exposure of cells to 2 or 4  $\mu\text{M}$  of  $\beta$ -lap with or without T2AA (20  $\mu\text{M}$ ). Increasing concentrations of  $\beta$ -lap resulted in increasing levels of  $\text{H}_2\text{O}_2$  a measurement of ROS production (Fig. 2B). The combination of  $\beta$ -lap (2 or 4  $\mu\text{M}$ ) with T2AA resulted in a significant increase in  $\text{H}_2\text{O}_2$  levels compared to  $\beta$ -lap treatment alone (Fig. 2B). Flow cytometric analysis confirmed elevated ROS formation by staining with DCFDA (Supplementary Fig. S2). Treatment with dicumarol (DIC, an NQO1-specific inhibitor, 50  $\mu\text{M}$ ) suppressed the combination treatment-induced ROS formation (Fig. 2B and Supplementary Fig. S2). Our findings suggest that inhibition of PCNA function by T2AA may amplify  $\beta$ -lap-induced DNA damage.

Our previous studies have demonstrated that exposure to  $\beta$ -lap causes DNA lesions in *NQO1*<sup>+</sup> NSCLC, breast cancer, and pancreatic cancer cells, resulting in PARP hyperactivation in terms of the accumulation of the poly(ADP-ribose)-PARP (PAR-PARP) posttranslational protein modification [9]. To investigate whether T2AA affects  $\beta$ -lap-induced PARP hyperactivation (PAR formation), MiaPaCa2 cells were exposed to 2  $\mu\text{M}$   $\beta$ -lap or 20  $\mu\text{M}$  T2AA alone or in combination for the measurement of PAR formation (Fig. 2C). Western blotting analysis and quantitation of the protein levels with NIH image J indicates that treatment with 2  $\mu\text{M}$   $\beta$ -lap resulted in increasing PAR protein levels from 5 to 120 minutes after treatment and the appearance of  $\gamma$ -H2AX protein, a surrogate for DNA double strand break formation, is induced at 30, 60, and 120 minutes post-treatment. Interestingly, the combination of 2  $\mu\text{M}$   $\beta$ -lap with T2AA resulted in a statistically significant decrease in PAR protein formation compared to  $\beta$ -lap alone, and PCNA inhibition by T2AA produced higher  $\gamma$ -H2AX protein levels when coadministered with  $\beta$ -lap (Fig. 2C). Furthermore, PCNA inhibition by T2AA enhanced  $\beta$ -lap-induced  $\text{NAD}^+$ /ATP loss in a dose-dependent manner, and DIC an NQO1 inhibitor rescued the combination treatment-induced catastrophic energy loss of  $\text{NAD}^+$ /ATP (Fig. 2D, E). Altogether, our findings suggest that PCNA inhibition by T2AA induces more ROS production and DNA damage that causes  $\text{NAD}^+$ /ATP depletion, leading to a decrease in PAR formation due to an exhaustion of the  $\text{NAD}^+$  pool.

### 3.3. Knockdown of PCNA expression decreases $\beta$ -lap-induced PAR formation and NAD<sup>+</sup>/ATP loss

To investigate whether it is indeed T2AA inhibition of PCNA that can explain the enhanced toxicity of low doses of  $\beta$ -lap when combined with treatment with T2AA, we used short interfering RNA (siRNA) to induce specific PCNA gene silencing in A549, MiaPaCa2, MDA-MB-231, A549/MiaPaCa2 NQO1-KO or MDA-MB-231-NQO1<sup>+</sup> cells and examined the impact on the  $\beta$ -lap antitumor effect with or without targeted PCNA gene knockdown. Many other studies have demonstrated that PCNA is intimately linked to DNA replication and DNA repair [25, 26]. First we found that knockdown of PCNA expression enhanced  $\beta$ -lap killing in NQO1<sup>+</sup> A549, MiaPaCa2 and MDA-MB-231-NQO1<sup>+</sup> cancer cells (Fig. 3A and Supplementary Fig. S3A, C), while knockout of NQO1 abolished this effect (Supplementary Fig. S3B, D). This result is quite similar to the response measured with cotreatment with  $\beta$ -lap + T2AA (Fig. 1A–C, E, H). Furthermore, in Figure 3B we show western blotting analysis and quantitation of A549 cells incubated with siSCR or siPCNA and then treated with or without 3  $\mu$ M  $\beta$ -lap at different time points within 2 h. As hypothesized, similar to previous western blotting results (Fig. 2C), significant suppression of  $\beta$ -lap-induced PAR formation was observed in siPCNA transfected A549 cells treated with 3  $\mu$ M  $\beta$ -lap (Fig. 3B), while  $\beta$ -lap-induced PAR formation was totally eliminated by siPCNA in A549-NQO1-KO cells (Supplementary Fig. S3E, F). These findings suggest that synergism of  $\beta$ -lap by PCNA inhibition is NQO1-dependent. Subsequent western blotting for  $\gamma$ -H2AX showed elevated and earlier DSB formation with siPCNA transfected compared with siSCR transfected A549 cells treated with 3  $\mu$ M  $\beta$ -lap (Fig. 3B), implying that inhibition of PCNA by siRNA knockdown or treatment with T2AA plays a major role in the enhancement of  $\beta$ -lap toxicity in NQO1<sup>+</sup> cancer cells. Knockout of PCNA expression in A549 cells was confirmed by western blotting analysis (Fig. 3B). It was shown above that addition of the PCNA inhibitor T2AA promoted intracellular NAD<sup>+</sup>/ATP consumption in wild-type NQO1<sup>+</sup> cells (Fig. 2D, E). Here, we investigated changes in NAD<sup>+</sup>/ATP levels in both siPCNA and siSCR treated NQO1<sup>+</sup> A549 cells. Relative ATP and NAD<sup>+</sup> levels were monitored after 2 h of  $\beta$ -lap (0–4  $\mu$ M) treatment (Fig. 3C, D). Interestingly, we observed inverse results: PCNA knockdown rescued  $\beta$ -lap-induced NAD<sup>+</sup>/ATP loss in contrast to wild-type expression in NQO1<sup>+</sup> cells treated with the PCNA inhibitor T2AA (Fig. 3C, D). These data suggest that as hypothesized knockdown of PCNA expression decreases  $\beta$ -lap-induced PAR formation and NAD<sup>+</sup>/ATP loss.

### 3.4. The combination of T2AA with $\beta$ -lap amplifies NQO1-dependent DNA damage

DNA DSBs have been shown to be a highly lethal form of DNA damage in human cells [42]. Here, we hypothesized that combination treatment of NQO1<sup>+</sup> cells with T2AA +  $\beta$ -lap would result in enhanced DSB formation due to significant DNA damage generation through induction of ROS, PARP1 hyperactivation, and the conversion of DNA single-strand lesions to DSBs. Here, we determined the DNA damage repair response through assessment of the formation of foci of the combined DSB surrogate markers  $\gamma$ -H2AX and 53BP1 in MiaPaCa2 cells. Treatment with T2AA (20  $\mu$ M, 4 h) alone or  $\beta$ -lap (2  $\mu$ M, 2 h) alone produced the formation of a small number (~10) of  $\gamma$ -H2AX and 53BP1 foci (Fig. 4A, B). In contrast, cotreatment with T2AA (20  $\mu$ M, 4 h) +  $\beta$ -lap (2  $\mu$ M, 2 h) resulted in a statistically significant increase in  $\gamma$ -H2AX and 53BP1 foci formation to (~25) (Fig. 4A, B).

$\beta$ -Lap (8  $\mu$ M, 2 h), leading to a hyperlethal effect, resulted in extensive DSB formation, and DIC blocked the formation of combination treatment-induced  $\gamma$ -H2AX and 53BP1 foci (Fig. 4A, B).

To obtain a more direct measure of DNA damage induction we performed alkaline denaturing comet assays to detect changes in cell nuclear DNA migration due to base damage, SSBs, and DSBs in the various treatment groups. Treatment of MiaPaCa2 cells with either 20  $\mu$ M of T2AA for 4 h or with 2  $\mu$ M of  $\beta$ -lap for 2 h alone induce relatively minor changes in comet tail length to  $10 \pm 2$  and  $20 \pm 5$  a.u. respectively versus controls  $7 \pm 2$  a.u. (Fig. 4C, D). However, the combination treatment with  $\beta$ -lap (2  $\mu$ M, 2 h) and T2AA (20  $\mu$ M, 4 h) resulted in a large and statistically significant enhancement of comet tail length to  $60 \pm 10$  a.u. compared to controls or individual single treatments. (Fig. 4C, D). The addition of the NQO1-specific inhibitor DIC suppressed the combination treatment-induced increase in comet tail length. Taken together the comet data indicate that inhibition of PCNA by T2AA amplifies  $\beta$ -lap-induced NQO1-dependent DNA damage.

### 3.5. PCNA inhibition by T2AA promotes programmed necrosis and G1/S phase cell cycle arrest in $\beta$ -lap-exposed NQO1<sup>+</sup> cancer cells

Treatment of MiaPaCa2 cells with a lethal dose of  $\beta$ -lap alone (8  $\mu$ M, 2 h) caused atypical 60 kDa PARP1 and 40 kDa P53 proteolytic cleavage (Fig. 5A, **lane 6**), which we have previously shown to be diagnostic of the induction programmed necrosis [9]. The combination treatment of 20  $\mu$ M T2AA + 2  $\mu$ M  $\beta$ -lap treatment on MiaPaCa2 cells resulted in weak atypical PARP1 cleavage and P53 cleavage compared to 8  $\mu$ M  $\beta$ -lap alone (Fig. 5A, **lanes 3 and 4**). Caspase activation was not detected in any of the treatment groups, and ZVAD-fmk (a caspase inhibitor) did not affect proteolysis or cell death (Fig. 5A, **lanes 5 and 7**). As an apoptotic positive control, we treated MiaPaCa2 cells with staurosporine (STS; 1  $\mu$ M, 18 h) and western blotting confirmed the appearance of 89 kDa PARP1 cleavage and caspase-3/7-mediated proteolysis (Fig. 5A, **lane 8**), indicating that apoptosis occurred in MiaPaCa2 cells exposed to STS. STS-induced cleavage was blocked by ZVAD-fmk (Fig. 5A, **lane 9**). We then further investigated the cell death pathway induced by combination treatment with T2AA and  $\beta$ -lap through PI/Annexin V-FITC staining by flow cytometry. Treatment with 20  $\mu$ M T2AA or 2  $\mu$ M  $\beta$ -lap alone led to a few MiaPaCa2 cells eventually undergoing necrotic death (Fig. 5B). However, combination treatment with 2  $\mu$ M  $\beta$ -lap and 20  $\mu$ M T2AA or treatment with a lethal dose of  $\beta$ -lap (8  $\mu$ M) resulted in a significant increase in necrotic cell death, and NQO1 inhibitor DIC partially suppressed this death (Fig. 5B). The results are consistent with the western blotting results (Fig. 5A). These data suggest that inhibition of PCNA by T2AA does not switch the cell death pathway but enhances the lethality of a sublethal dose of  $\beta$ -lap (2  $\mu$ M) due to an increase in necrosis.

Our previous studies have demonstrated that  $\beta$ -lap-induced NQO1<sup>+</sup> cancer cell death is independent of cell cycle phases [22]. To investigate whether inhibition of PCNA by T2AA has an effect on the NQO1<sup>+</sup> cancer cell cycle phase, the percentages of cells in the G1, S and G2 phases of the cell cycle were measured by EdU and PI staining and then summarized by flow cytometry. Treatment with 2  $\mu$ M  $\beta$ -lap alone had no impact on the percentages of cells in the G1, S and G2 phases compared to control treatment (DMSO) (Fig. 5C). However,

20  $\mu\text{M}$  T2AA alone evidently led to cell arrest in the G1/S phase and the combination of  $\beta$ -lap with T2AA further enhanced G1/S phase cell cycle arrest (Fig. 5C). In summary, our findings revealed that T2AA suppresses the proliferation of *NQO1*<sup>+</sup> cancer cells by causing G1/S phase cell cycle arrest with the induction and promotion of programmed necrosis.

### 3.6. Combination treatment enhances super-additive antitumor activity in subcutaneous LLC models

To test the *in vivo* efficacy of the PCNA inhibitor  $\pm$   $\beta$ -lap treatment in murine Lewis lung carcinoma (LLC) tumor-bearing mice, we first investigate whether  $\beta$ -lap synergizes with PCNA inhibitor T2AA in murine LLC cells ( $\sim 50$  unit/mg tissue of NQO1 enzyme activity) [13]. We examined the cell viability of  $\beta$ -lap  $\pm$  T2AA with or without DIC (50  $\mu\text{M}$ ) in LLC cells and found that, similar to the results in Figure 1,  $\beta$ -lap's cytotoxicity was enhanced by T2AA in LLC cells and this effect was NQO1-dependent (Fig. 6A). Nontoxic dose of PCNA inhibitor T2AA in LLC cells was also screened (Supplementary Fig. S4).

Next, mice were inoculated subcutaneously with  $\sim 2 \times 10^6$  murine LLC cells and monitored for tumor formation. When tumor volume reached 50–80  $\text{cm}^3$ , mice were randomly divided into four groups ( $n=8/\text{group}$ ) and treated with vehicle (HP $\beta$ CD, intratumorally injection [i.t.]), HP $\beta$ CD- $\beta$ -lap (18 mg/kg, i.t.) or HP $\beta$ CD-T2AA (20 mg/kg, i.t.) alone, or HP $\beta$ CD-T2AA (20 mg/kg, i.t.) 1 h prior to HP $\beta$ CD- $\beta$ -lap (18 mg/kg, i.t.). Treatments were given once per day for five consecutive days. Two days later, another 5 treatments were repeated. Mice were then monitored for changes in tumor volumes (Fig. 6B) and overall survival (Fig. 6C). The results showed that non-toxic dose of T2AA had no significant tumor-suppressive effects, while  $\beta$ -lap alone resulted in decreased tumor growth and increased survival rate of murine LLC tumor-bearing mice, although all mice succumbed to tumor burden by day 24 (Fig. 6B, C). In contrast, mice treated with T2AA +  $\beta$ -lap showed enhanced antitumor activity and significant survival benefit compared to these two single agents alone (Fig. 6B, C).

## 4. Discussion

In this study, we show that combining PCNA inhibition with a highly tumor-specific damaging agent,  $\beta$ -lap, leads to synergistic antitumor effect with non-toxic doses of both drugs in NQO1-overexpressing cancer cells.  $\beta$ -Lap + T2AA treatment results in robust, NQO1-dependent and tumor-selective induction of ROS formation and programmed necrosis both *in vitro* and *in vivo*. Mechanistically, as shown in Fig. 6D,  $\beta$ -Lap is reduced by NQO1 in the presence of NAD(P)H, resulting in superoxide (ROS) formation, which then induces DNA damage leading to PAR formation that results in NAD<sup>+</sup>/ATP depletion, and cells undergo tumor selective, NQO1-dependent programmed necrosis. However, when  $\beta$ -lap combines with PCNA inhibition (T2AA/siPCNA), the PCNA inhibition decreases  $\beta$ -lap-induced PARP1 hyperactivation and increases ROS production, which results in greater DNA damage and G1/S cell cycle arrest. This combination therapy enhances the lethality of a sublethal dose of  $\beta$ -lap (2  $\mu\text{M}$ ) due to a dramatic increase in DNA DSBs.

Numerous studies have revealed that  $\beta$ -lap is a highly tumor-specific competent NQO1-bioactivatable agent that is a promising candidate for targeted cancer therapy [13, 43].

However, inevitable deficiencies have limited further clinical applications. Here, we hypothesized that these hurdles might be overcome by combining the PCNA inhibitor T2AA with  $\beta$ -lap, resulting in synergistic antitumor effects when both are used at nontoxic doses to treat various *NQO1*<sup>+</sup> cancer cells. We hoped to improve the lethality of  $\beta$ -lap and decrease its acute toxicity with the aid of T2AA to appropriately exploit  $\beta$ -lap utilization.

We first demonstrated in this study that  $\beta$ -lap could achieve efficacious synergistic toxicity by combination with the PCNA inhibitor T2AA in *NQO1*<sup>+</sup>-overexpressing breast, pancreatic, and NSC lung cancer cells (Fig. 1A–H). We then showed by genetic KO and reconstitution of *NQO1* that this synergism was NQO1 dependent in all three cancer cell types (Fig. 1A–H), and then investigated the mechanisms involved. Analyses of the Oxygen Consumption Ratio (OCR) for cells treated with increasing concentrations of  $\beta$ -lap alone showed the expected rapid increase in OCR, which we have previously shown to be indicative of cells undergoing an NQO1-dependent futile redox cycle that depletes the *NQO1*<sup>+</sup> cancer cells NAD<sup>+</sup>/ATP energy stores inducing cell death [9]. These increases in OCR were particularly evident at the highly toxic 4 and 8  $\mu$ M  $\beta$ -lap treatments (Fig. 2A). Treatment with a nontoxic 20  $\mu$ M dose of T2AA did not significantly alter OCR versus controls. However, the combination of 20  $\mu$ M T2AA and 8  $\mu$ M of  $\beta$ -lap reduced the OCR observed versus treatment with 8  $\mu$ M of  $\beta$ -lap alone. (Fig. 2A). We hypothesized that this reduction in OCR was due to T2AA inhibition of the PCNA protein which is involved in DNA replication and repair processes that consume large amounts of oxygen [44]. However, the mechanism of why the combination of nontoxic doses of T2AA and  $\beta$ -lap killed *NQO1*<sup>+</sup> cancer cells needed to be clarified. We hypothesized that the increased synergistic kill observed with the combination of T2AA and  $\beta$ -lap could be due to an increase in damage to DNA caused by an increase in reactive oxygen species (ROS). We found clear evidence that treatment with 2 or 4  $\mu$ M  $\beta$ -lap increased the production of ROS over controls and T2AA treated cancer cells alone, and that the addition 20  $\mu$ M T2AA further increased the production of ROS over treatment with 2 or 4  $\mu$ M  $\beta$ -lap alone. Treatment with 50  $\mu$ M DIC (an NQO1-specific inhibitor) suppressed the induction of ROS by 2 and 4  $\mu$ M  $\beta$ -lap treatment as well as by the combination treatment of 2 or 4  $\mu$ M  $\beta$ -lap plus 20  $\mu$ M T2AA (Fig. 2B). The elevation in ROS production observed by combined suggested a potential mechanism for the observed synergism in killing when *NQO1*<sup>+</sup> cancer cells are treated with 2 and 4  $\mu$ M  $\beta$ -lap combined with 20  $\mu$ M T2AA (Fig. 2B). Notably, the addition of T2AA decreased the synthesis of PAR, which correlated with accelerated and increased cell death (Fig. 2C). Furthermore, the addition of T2AA with 2 and 4  $\mu$ M  $\beta$ -lap treatment enhanced depletion cellular energy reserves measured by NAD<sup>+</sup> and ATP measurements. Finally, treatment with 50  $\mu$ M DIC (an NQO1-specific inhibitor) suppressed the reductions of NAD<sup>+</sup> and ATP suggesting that the drug combination reduction in cellular energy stores retained NQO1 dependency (Fig. 2D, E).

We hypothesized that the synergism in toxicity observed with  $\beta$ -lap and T2AA in *NQO1*<sup>+</sup> tumor cells was due to T2AA inhibition of PCNA activity. We tested this hypothesis by knocking down PCNA with siRNA versus scramble control siSCR in A549 cells (Fig. 3A–C). We clearly show that PCNA silencing led to cells being highly hypersensitive to low dose  $\beta$ -lap treatment (Fig. 3A). In addition, siRNA knockdown of PCNA reduced PAR formation induced by treatment with 3  $\mu$ M  $\beta$ -lap (Fig. 3A) and increased the induction

of DNA damage measured by  $\gamma$ H2AX foci formation and comet assays (Figs. 3B). These data support our hypothesis that inhibition of PCNA by T2AA treatments increases cancer cell death by increasing  $\beta$ -lap-induced ROS and SSB and DSB DNA damage (Fig. 4). Furthermore, western blotting and flow cytometric analysis show that treatment with  $\beta$ -lap + T2AA double the percentage of cells undergoing programmed necrosis compared to cancer cells treated with  $\beta$ -lap alone (Fig. 5). Finally, we show by DNA flow cytometry histogram analysis that treatment with the PCNA inhibitor T2AA induces a strong G1/S block and that the addition of  $\beta$ -lap enhances the induction of this G1/S block (Fig. 5C). We proposed that since PCNA is a processivity factor for enhancing the binding of DNA polymerases to the DNA template during the S (DNA synthesis) phase of the cell cycle [45], the inhibition of PCNA results in an antiproliferative blocking effect and inhibits progression into and through S phase in *NQO1*<sup>+</sup> cells (Fig. 5C).

Interestingly, knockdown of PCNA by siRNA reduced the observed relative suppression in both NAD<sup>+</sup> and ATP levels in A549 lung cancer cells treated with 1, 2, 3, or 4  $\mu$ M  $\beta$ -lap versus A549 lung cancer treated with the scramble siRNA control (Fig. 3C, D). We speculate that the reduced reduction in NAD<sup>+</sup> and ATP levels by  $\beta$ -lap treatment in A549 cells after siRNA knocked down PCNA can be explained by PCNA's role in DNA replication by the DNA replication factor C (RFC) which is a five-subunit protein complex needed for DNA replication [46]. Data indicates that the ATP hydrolysis activity of RFC is essential for the formation of a functional PCNA clamp loader on the DNA [47, 48]. We propose that siRNA PCNA knockdown leads to a reduction in this ATP hydrolysis, and results in relatively higher levels of NAD<sup>+</sup> and ATP when cells are treated with 1, 2, 3, or 4  $\mu$ M  $\beta$ -lap.

Our *in vitro* observations strongly indicate the efficacy of combining nontoxic doses of  $\beta$ -lap with PCNA inhibitor T2AA to kill a variety of *NQO1*<sup>+</sup> cancer cell types. More importantly, the antitumor effect of combination of  $\beta$ -lap with T2AA is further demonstrated in our *in vivo* study in Lewis lung carcinoma (LLC)-tumor-bearing mice (Fig. 6B, C).

To date, researchers have not been content with simple  $\beta$ -lap monotherapy studies. Instead, they are investing more effort than ever in exploiting  $\beta$ -lap-related combination therapy and immunotherapy [9, 13, 49]. In this study, we investigated and clearly demonstrated the efficacy of combining nontoxic doses of  $\beta$ -lap and the PCNA inhibitor T2AA to kill a variety of *NQO1*<sup>+</sup> cancer cell types and the mechanism of the enhance toxicity which involved increased ROS production and enhanced DNA damage that enhanced cell death by programmed necrosis. These novel results provide new insight into potential combination  $\beta$ -lap-relevant therapy with PCNA inhibitors in *NQO1*<sup>+</sup> cancers. We anticipate that  $\beta$ -lap + T2AA combined treatment could be a particularly efficacious tumor-selective therapy against a wide range of *NQO1*<sup>+</sup> solid cancers. Importantly, our data suggest that  $\beta$ -lap + PCNA inhibitor therapy may be efficacious at nontoxic individual doses of  $\beta$ -lap and T2AA thereby reducing dose-limiting toxicities and side effects.

## Supplementary Material

Refer to Web version on PubMed Central for supplementary material.

## Funding

This work was supported by NIH R01 grants CA221158, CA224493 and CA240952 to X. Huang. This work was also supported by the IU Simon Comprehensive Cancer Center (Grant P30CA082709).

## Abbreviations

|                                   |                                    |
|-----------------------------------|------------------------------------|
| <b>NQO1</b>                       | NAD(P)H: quinone oxidoreductase-1  |
| <b>β-Lap</b>                      | β-Lapachone                        |
| <b>PCNA</b>                       | proliferating cell nuclear antigen |
| <b>T2AA</b>                       | T2 amino alcohol                   |
| <b>DSB</b>                        | double-strand break                |
| <b>ROS</b>                        | reactive oxygen species            |
| <b>ER</b>                         | endoplasmic reticulum              |
| <b>SSBR</b>                       | single-strand break repair         |
| <b>HR</b>                         | homologous recombination           |
| <b>NHEJ</b>                       | nonhomologous end joining          |
| <b>BER</b>                        | base excision repair               |
| <b>RFC</b>                        | replication factor C               |
| <b>NSCLC</b>                      | Non-small cell lung cancer         |
| <b>PDA</b>                        | pancreatic adenocarcinoma          |
| <b>ATCC</b>                       | American Tissue Culture Collection |
| <b>DMEM</b>                       | Dulbecco's modified Eagle's medium |
| <b>FBS</b>                        | fetal bovine serum                 |
| <b>DIC</b>                        | dicoumarol                         |
| <b>H<sub>2</sub>O<sub>2</sub></b> | hydrogen peroxide                  |
| <b>FCM</b>                        | flow cytometry                     |
| <b>SSBs</b>                       | single-strand breaks               |
| <b>PI</b>                         | propidium iodide                   |
| <b>EdU</b>                        | 5-ethynyl-2'-deoxyuridine          |
| <b>STS</b>                        | staurosporine                      |
| <b>DMSO</b>                       | Dimethyl sulfoxide                 |

|                        |                                   |
|------------------------|-----------------------------------|
| <b>ATP</b>             | Adenosine triphosphate            |
| <b>NAD<sup>+</sup></b> | nicotinamide adenine dinucleotide |

## References

- [1]. Cao Y, Adipocyte and lipid metabolism in cancer drug resistance, *J Clin Invest*, 129 (2019) 3006–3017. [PubMed: 31264969]
- [2]. Li X, Wenes M, Romero P, Huang SC, Fendt SM, Ho PC, Navigating metabolic pathways to enhance antitumour immunity and immunotherapy, *Nat Rev Clin Oncol*, 16 (2019) 425–441. [PubMed: 30914826]
- [3]. Siegel RL, Miller KD, Jemal A, Cancer statistics, 2020, *CA: a cancer journal for clinicians*, 70 (2020) 7–30. [PubMed: 31912902]
- [4]. Piawah S, Venook AP, Targeted therapy for colorectal cancer metastases: A review of current methods of molecularly targeted therapy and the use of tumor biomarkers in the treatment of metastatic colorectal cancer, *Cancer*, 125 (2019) 4139–4147. [PubMed: 31433498]
- [5]. Chen S, Cao Q, Wen W, Wang H, Targeted therapy for hepatocellular carcinoma: Challenges and opportunities, *Cancer Lett*, 460 (2019) 1–9. [PubMed: 31207320]
- [6]. Bey EA, Bentle MS, Reinicke KE, Dong Y, Yang CR, Girard L, Minna JD, Bornmann WG, Gao J, Boothman DA, An NQO1- and PARP-1-mediated cell death pathway induced in non-small-cell lung cancer cells by beta-lapachone, *Proc Natl Acad Sci U S A*, 104 (2007) 11832–11837. [PubMed: 17609380]
- [7]. Cao L, Li LS, Spruell C, Xiao L, Chakrabarti G, Bey EA, Reinicke KE, Srougi MC, Moore Z, Dong Y, Vo P, Kabbani W, Yang CR, Wang X, Fattah F, Morales JC, Motea EA, Bornmann WG, Yordy JS, Boothman DA, Tumor-selective, futile redox cycle-induced bystander effects elicited by NQO1 bioactivatable radiosensitizing drugs in triple-negative breast cancers, *Antioxid Redox Signal*, 21 (2014) 237–250. [PubMed: 24512128]
- [8]. Dong Y, Bey EA, Li LS, Kabbani W, Yan J, Xie XJ, Hsieh JT, Gao J, Boothman DA, Prostate cancer radiosensitization through poly(ADP-Ribose) polymerase-1 hyperactivation, *Cancer Res*, 70 (2010) 8088–8096. [PubMed: 20940411]
- [9]. Huang X, Motea EA, Moore ZR, Yao J, Dong Y, Chakrabarti G, Kilgore JA, Silvers MA, Patidar PL, Cholka A, Fattah F, Cha Y, Anderson GG, Kusko R, Peyton M, Yan J, Xie XJ, Sarode V, Williams NS, Minna JD, Beg M, Gerber DE, Bey EA, Boothman DA, Leveraging an NQO1 Bioactivatable Drug for Tumor-Selective Use of Poly(ADP-ribose) Polymerase Inhibitors, *Cancer Cell*, 30 (2016) 940–952. [PubMed: 27960087]
- [10]. Li LS, Bey EA, Dong Y, Meng J, Patra B, Yan J, Xie XJ, Brekken RA, Barnett CC, Bornmann WG, Gao J, Boothman DA, Modulating endogenous NQO1 levels identifies key regulatory mechanisms of action of  $\beta$ -lapachone for pancreatic cancer therapy, *Clin Cancer Res*, 17 (2011) 275–285. [PubMed: 21224367]
- [11]. Kee JY, Han YH, Kim DS, Mun JG, Park SH, So HS, Park SJ, Park R, Um JY, Hong SH,  $\beta$ -Lapachone suppresses the lung metastasis of melanoma via the MAPK signaling pathway, *PLoS One*, 12 (2017) e0176937. [PubMed: 28481901]
- [12]. Park JS, Leem YH, Park JE, Kim DY, Kim HS, Neuroprotective Effect of  $\beta$ -Lapachone in MPTP-Induced Parkinson's Disease Mouse Model: Involvement of Astroglial p-AMPK/Nrf2/HO-1 Signaling Pathways, *Biomol Ther (Seoul)*, 27 (2019) 178–184. [PubMed: 30739428]
- [13]. Motea EA, Huang X, Singh N, Kilgore JA, Williams NS, Xie XJ, Gerber DE, Beg MS, Bey EA, Boothman DA, NQO1-dependent, Tumor-selective Radiosensitization of Non-small Cell Lung Cancers, *Clin Cancer Res*, 25 (2019) 2601–2609. [PubMed: 30617135]
- [14]. Lamberti MJ, Morales Vasconsuelo AB, Chiaramello M, Ferreira VF, Macedo Oliveira M, Baptista Ferreira S, Rivarola VA, Rumie Vittar NB, NQO1 induction mediated by photodynamic therapy synergizes with  $\beta$ -Lapachone-halogenated derivative against melanoma, *Biomed Pharmacother*, 108 (2018) 1553–1564. [PubMed: 30372857]
- [15]. Moore Z, Chakrabarti G, Luo X, Ali A, Hu Z, Fattah FJ, Vemireddy R, DeBerardinis RJ, Brekken RA, Boothman DA, NAMPT inhibition sensitizes pancreatic adenocarcinoma cells to

tumor-selective, PAR-independent metabolic catastrophe and cell death induced by  $\beta$ -lapachone, *Cell Death Dis*, 6 (2015) e1599. [PubMed: 25590809]

- [16]. Huang X, Dong Y, Bey EA, Kilgore JA, Bair JS, Li LS, Patel M, Parkinson EI, Wang Y, Williams NS, Gao J, Hergenrother PJ, Boothman DA, An NQO1 substrate with potent antitumor activity that selectively kills by PARP1-induced programmed necrosis, *Cancer Res*, 72 (2012) 3038–3047. [PubMed: 22532167]
- [17]. Kahanda D, Chakrabarti G, McWilliams MA, Boothman DA, Slinker JD, Using DNA devices to track anticancer drug activity, *Biosens Bioelectron*, 80 (2016) 647–653. [PubMed: 26901461]
- [18]. Nita M, Grzybowski A, The Role of the Reactive Oxygen Species and Oxidative Stress in the Pathomechanism of the Age-Related Ocular Diseases and Other Pathologies of the Anterior and Posterior Eye Segments in Adults, *Oxid Med Cell Longev*, 2016 (2016) 3164734. [PubMed: 26881021]
- [19]. Bentle MS, Reinicke KE, Bey EA, Spitz DR, Boothman DA, Calcium-dependent modulation of poly(ADP-ribose) polymerase-1 alters cellular metabolism and DNA repair, *J Biol Chem*, 281 (2006) 33684–33696. [PubMed: 16920718]
- [20]. Munoz FM, Zhang F, Islas-Robles A, Lau SS, Monks TJ, From the Cover: ROS-Induced Store-Operated Ca<sup>2+</sup> Entry Coupled to PARP-1 Hyperactivation Is Independent of PARG Activity in Necrotic Cell Death, *Toxicol Sci*, 158 (2017) 444–453. [PubMed: 28525621]
- [21]. Mashimo M, Kato J, Moss J, ADP-ribosyl-acceptor hydrolase 3 regulates poly (ADP-ribose) degradation and cell death during oxidative stress, *Proc Natl Acad Sci U S A*, 110 (2013) 18964–18969. [PubMed: 24191052]
- [22]. Bentle MS, Reinicke KE, Dong Y, Bey EA, Boothman DA, Nonhomologous end joining is essential for cellular resistance to the novel antitumor agent, beta-lapachone, *Cancer Res*, 67 (2007) 6936–6945. [PubMed: 17638905]
- [23]. Dias RB, de Araújo TBS, de Freitas RD, Rodrigues A, Sousa LP, Sales CBS, Valverde LF, Soares MBP, Dos Reis MG, Coletta RD, Ramos EAG, Camara CA, Silva TMS, Filho JMB, Bezerra DP, Rocha CAG,  $\beta$ -Lapachone and its iodine derivatives cause cell cycle arrest at G(2)/M phase and reactive oxygen species-mediated apoptosis in human oral squamous cell carcinoma cells, *Free radical biology & medicine*, 126 (2018) 87–100. [PubMed: 30071298]
- [24]. Tseng CH, Cheng CM, Tzeng CC, Peng SI, Yang CL, Chen YL, Synthesis and anti-inflammatory evaluations of  $\beta$ -lapachone derivatives, *Bioorg Med Chem*, 21 (2013) 523–531. [PubMed: 23232148]
- [25]. Choe KN, Moldovan GL, Forging Ahead through Darkness: PCNA, Still the Principal Conductor at the Replication Fork, *Mol Cell*, 65 (2017) 380–392. [PubMed: 28157503]
- [26]. Prestel A, Wichmann N, Martins JM, Marabini R, Kassem N, Broendum SS, Otterlei M, Nielsen O, Willemoës M, Ploug M, Boomsma W, Kragelund BB, The PCNA interaction motifs revisited: thinking outside the PIP-box, *Cell Mol Life Sci*, 76 (2019) 4923–4943. [PubMed: 31134302]
- [27]. Sisakova A, Altmannova V, Sebesta M, Krejci L, Role of PCNA and RFC in promoting Mus81-complex activity, *BMC Biol*, 15 (2017) 90. [PubMed: 28969641]
- [28]. Dilley RL, Verma P, Cho NW, Winters HD, Wondisford AR, Greenberg RA, Break-induced telomere synthesis underlies alternative telomere maintenance, *Nature*, 539 (2016) 54–58. [PubMed: 27760120]
- [29]. Davarnejad H, Joshi M, Ait-Hamou N, Munro K, Couture JF, ATXR5/6 Forms Alternative Protein Complexes with PCNA and the Nucleosome Core Particle, *J Mol Biol*, 431 (2019) 1370–1379. [PubMed: 30826376]
- [30]. Streich FC Jr., Lima CD, Capturing a substrate in an activated RING E3/E2-SUMO complex, *Nature*, 536 (2016) 304–308. [PubMed: 27509863]
- [31]. Inoue A, Kikuchi S, Hishiki A, Shao Y, Heath R, Evison BJ, Actis M, Canman CE, Hashimoto H, Fujii N, A small molecule inhibitor of monoubiquitinated Proliferating Cell Nuclear Antigen (PCNA) inhibits repair of interstrand DNA cross-link, enhances DNA double strand break, and sensitizes cancer cells to cisplatin, *J Biol Chem*, 289 (2014) 7109–7120. [PubMed: 24474685]
- [32]. PUNCHIHEWA C, Inoue A, Hishiki A, Fujikawa Y, Connelly M, Evison B, Shao Y, Heath R, Kuraoka I, Rodrigues P, Hashimoto H, Kawanishi M, Sato M, Yagi T, Fujii N, Identification of small molecule proliferating cell nuclear antigen (PCNA) inhibitor that disrupts interactions

- with PIP-box proteins and inhibits DNA replication, *J Biol Chem*, 287 (2012) 14289–14300. [PubMed: 22383522]
- [33]. Yang RY, Kizer D, Wu H, Volckova E, Miao XS, Ali SM, Tandon M, Savage RE, Chan TC, Ashwell MA, Synthetic methods for the preparation of ARQ 501 (beta-Lapachone) human blood metabolites, *Bioorg Med Chem*, 16 (2008) 5635–5643. [PubMed: 18424157]
- [34]. Pardee AB, Li YZ, Li CJ, Cancer therapy with beta-lapachone, *Curr Cancer Drug Targets*, 2 (2002) 227–242. [PubMed: 12188909]
- [35]. Wilson RH, Biasutto AJ, Wang L, Fischer R, Baple EL, Crosby AH, Mancini EJ, Green CM, PCNA dependent cellular activities tolerate dramatic perturbations in PCNA client interactions, *DNA Repair (Amst)*, 50 (2017) 22–35. [PubMed: 28073635]
- [36]. Pink JJ, Planchon SM, Tagliarino C, Varnes ME, Siegel D, Boothman DA, NAD(P)H:Quinone oxidoreductase activity is the principal determinant of beta-lapachone cytotoxicity, *J Biol Chem*, 275 (2000) 5416–5424. [PubMed: 10681517]
- [37]. Schluterman MK, Chapman SL, Korpanty G, Ozumi K, Fukai T, Yanagisawa H, Brekken RA, Loss of fibulin-5 binding to beta1 integrins inhibits tumor growth by increasing the level of ROS, *Dis Model Mech*, 3 (2010) 333–342. [PubMed: 20197418]
- [38]. Motea EA, Fattah FJ, Xiao L, Girard L, Rommel A, Morales JC, Patidar P, Zhou Y, Porter A, Xie Y, Minna JD, Boothman DA, Kub5-Hera (RPRD1B) Deficiency Promotes “BRCAness” and Vulnerability to PARP Inhibition in BRCA-proficient Breast Cancers, *Clin Cancer Res*, 24 (2018) 6459–6470. [PubMed: 30108102]
- [39]. Bey EA, Reinicke KE, Srougi MC, Varnes M, Anderson VE, Pink JJ, Li LS, Patel M, Cao L, Moore Z, Rommel A, Boatman M, Lewis C, Euhus DM, Bornmann WG, Buchsbaum DJ, Spitz DR, Gao J, Boothman DA, Catalase abrogates  $\beta$ -lapachone-induced PARP1 hyperactivation-directed programmed necrosis in NQO1-positive breast cancers, *Mol Cancer Ther*, 12 (2013) 2110–2120. [PubMed: 23883585]
- [40]. Torrente L, Prieto-Farigua N, Falzone A, Elkins CM, Boothman DA, Haura EB, DeNicola GM, Inhibition of TXNRD or SOD1 overcomes NRF2-mediated resistance to  $\beta$ -lapachone, *Redox Biol*, 30 (2020) 101440. [PubMed: 32007910]
- [41]. Chou TC, Talalay P, Quantitative analysis of dose-effect relationships: the combined effects of multiple drugs or enzyme inhibitors, *Adv Enzyme Regul*, 22 (1984) 27–55. [PubMed: 6382953]
- [42]. Lieber MR, The mechanism of double-strand DNA break repair by the nonhomologous DNA end-joining pathway, *Annu Rev Biochem*, 79 (2010) 181–211. [PubMed: 20192759]
- [43]. Wu X, Kasselouri A, Vergnaud-Gauduchon J, Rosilio V, Assessment of various formulation approaches for the application of beta-lapachone in prostate cancer therapy, *Int J Pharm*, 579 (2020) 119168. [PubMed: 32087264]
- [44]. Ng N, Purshouse K, Foskolou IP, Olcina MM, Hammond EM, Challenges to DNA replication in hypoxic conditions, *Febs j*, 285 (2018) 1563–1571. [PubMed: 29288533]
- [45]. Boehm EM, Gildenberg MS, Washington MT, The Many Roles of PCNA in Eukaryotic DNA Replication, *Enzymes*, 39 (2016) 231–254. [PubMed: 27241932]
- [46]. Reynolds N, Fantes PA, MacNeill SA, A key role for replication factor C in DNA replication checkpoint function in fission yeast, *Nucleic Acids Res*, 27 (1999) 462–469. [PubMed: 9862966]
- [47]. Majka J, Burgers PM, The PCNA-RFC families of DNA clamps and clamp loaders, *Prog Nucleic Acid Res Mol Biol*, 78 (2004) 227–260. [PubMed: 15210332]
- [48]. Sakato M, Zhou Y, Hingorani MM, ATP binding and hydrolysis-driven rate-determining events in the RFC-catalyzed PCNA clamp loading reaction, *J Mol Biol*, 416 (2012) 176–191. [PubMed: 22197378]
- [49]. Li X, Liu Z, Zhang A, Han C, Shen A, Jiang L, Boothman DA, Qiao J, Wang Y, Huang X, Fu YX, NQO1 targeting prodrug triggers innate sensing to overcome checkpoint blockade resistance, *Nat Commun*, 10 (2019) 3251. [PubMed: 31324798]

Synergy with PCNA inhibition and  $\beta$ -lapachone is NQO1 dependent

PCNA inhibitor +  $\beta$ -lapachone prevent DNA repair and increase DNA lesions and energy loss

PCNA inhibitor +  $\beta$ -lapachone promote programmed necrosis and G1/S phase cell cycle arrest

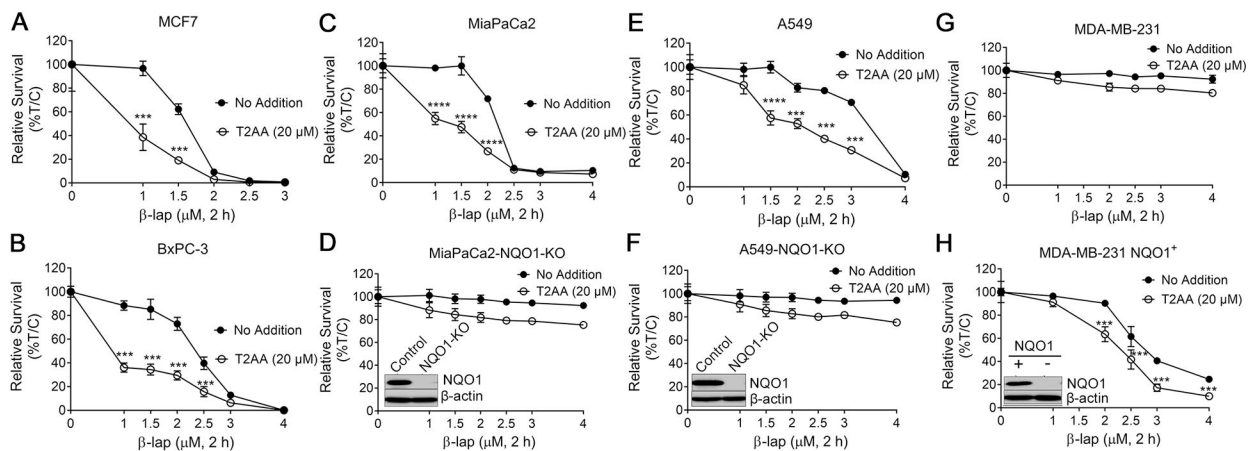


**Fig. 1. T2AA enhanced  $\beta$ -lap lethality in various types of NQO1-overexpressing cancer cells (A-H)** MCF-7 breast cancer cells, BxPC-3 PDA cells, MiaPaCa2 PDA cells, MiaPaCa2-NQO1-KO PDA cells, A549 NSCLC cells, A549-NQO1-KO NSCLC cells, MDA-MB-231 NQO1<sup>+</sup> breast cancer cells and MDA-MB-231 breast cancer cells were pretreated with or without T2AA (20  $\mu$ M, 2 h), then exposed or not to T2AA (20  $\mu$ M) +  $\beta$ -lap (0 – 4.0  $\mu$ M) for 2 h,  $\pm$  DIC (50  $\mu$ M). Drugs were removed and cell viability was determined by relative survival assay (DNA assay) 7 days later. All error bars represent the mean  $\pm$  SD. \*\*\*  $p < 0.001$ , \*\*  $p < 0.01$ , \*  $p < 0.05$  (t tests).

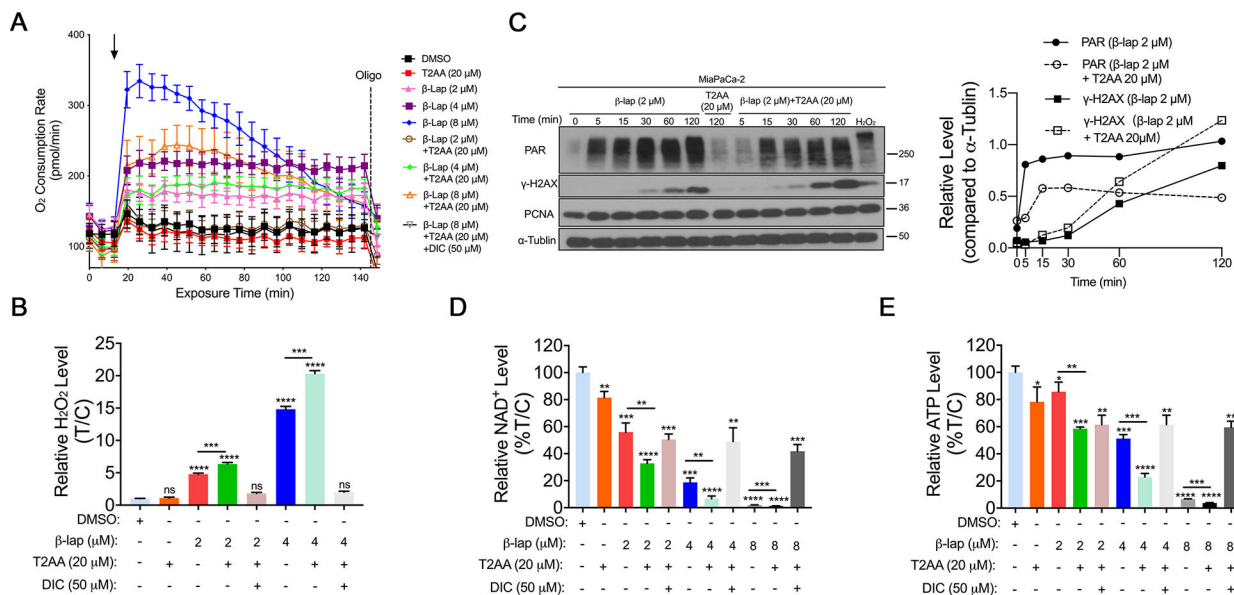


**Fig. 2. Inhibition of PCNA by T2AA causes NQO1-dependent PARP1 hyperactivation, ROS formation and NAD<sup>+</sup>/ATP loss**

(A) MiaPaCa2 PDA cells were pretreated with T2AA (20 μM, 2 h) and then treated with or without T2AA (20 μM, 2 h) + β-lap (2, 4 or 8 μM) ± DIC (50 μM) for 2 h. Cells were also treated with β-lap (2, 4 or 8 μM, 2 h). Real-time oxygen consumption rates (OCRs) after various drug treatments determined by Seahorse XF analyses. (B) H<sub>2</sub>O<sub>2</sub> level in each group at 2 h. (C) MiaPaCa2 PDA cells were pretreated with or without T2AA (20 μM, 2 h) and then cotreated with or without T2AA (20 μM, 2 h) + β-lap (2 μM) for 2 h. In addition, whole-cell lysates were prepared at the times indicated. Samples were assessed for PAR formation, γ-H2AX, PCNA and α-tubulin (loading control). Cells were also treated with H<sub>2</sub>O<sub>2</sub> (500 μM, 15 min) as the positive control. (D, E) MiaPaCa2 PDA cells were pretreated with or without T2AA (20 μM, 2 h) and then exposed or not to T2AA (20 μM, 2 h) + β-lap (2, 4 and 8 μM) ± DIC (50 μM) for 2 h. Cells were also treated with T2AA (20 μM, 48 h). Then, the relative NAD<sup>+</sup> and ATP levels were monitored. Results were separately repeated at least three times in triplicate. Results (mean ± SD) are from three independent experiments. \*\*\**p* < 0.001, \*\**p* < 0.01, \**p* < 0.05 (t test).

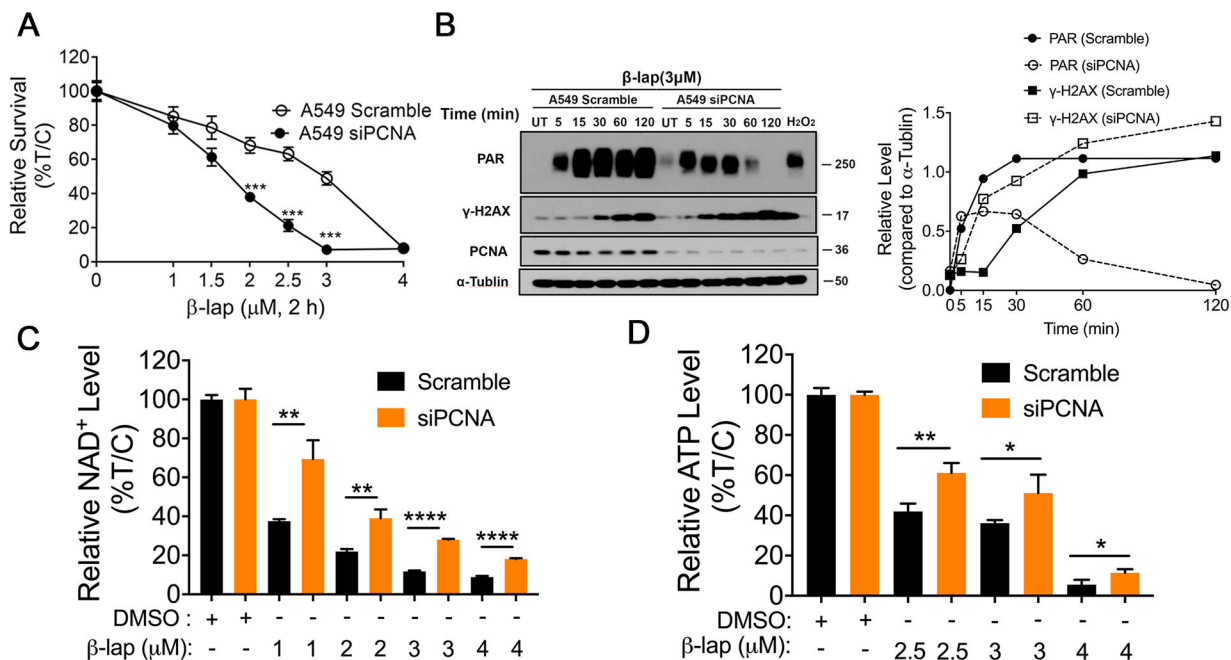


**Fig. 3. Knockdown of PCNA blocks DNA repair and NAD<sup>+</sup>/ATP consumption**

Transient siSCR or siPCNA A549 cells were treated with various concentrations of  $\beta$ -lap ( $\mu$ M) for 2 h. (A) Relative survival was then assessed. (B) SiSCR or siPCNA A549 cells were treated with  $\beta$ -lap (3  $\mu$ M), and whole-cell lysates were prepared at the times indicated. Samples were evaluated for PAR formation,  $\gamma$ -H2AX, NQO1 and  $\alpha$ -tubulin (loading control). SiPCNA was generated, and knockdown was confirmed by Western blotting. Cells were also treated with 500  $\mu$ M H<sub>2</sub>O<sub>2</sub> for 15 min as the positive control. Results were separately repeated at least three times in triplicate. (C, D) Relative ATP and NAD<sup>+</sup> levels were monitored. Results (mean  $\pm$  SD) are from three independent experiments. \*\*\* $p$  < 0.001, \*\* $p$  < 0.01, \* $p$  < 0.05 (t tests).

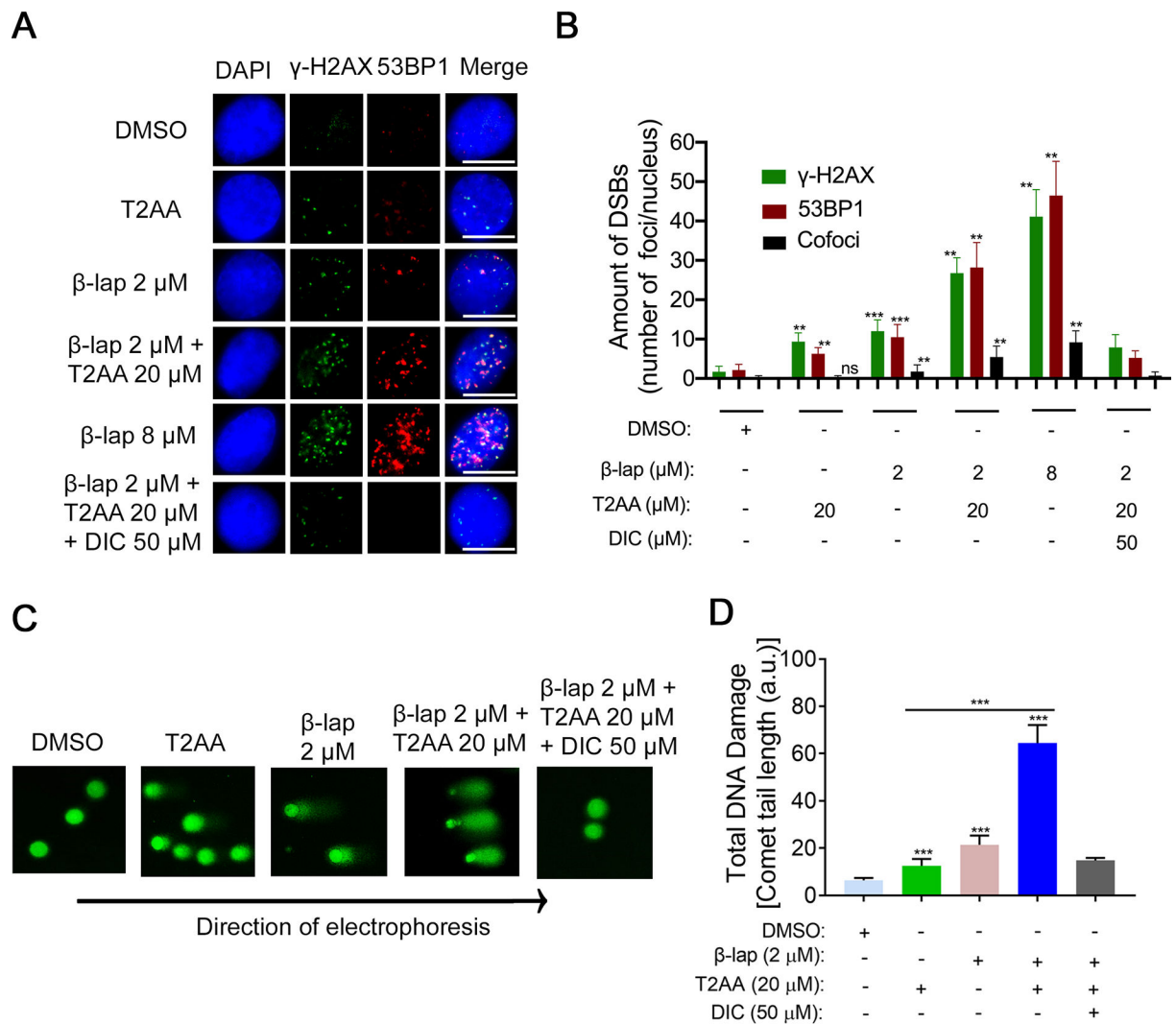


**Fig. 4. T2AA increases  $\beta$ -lap-induced DNA damage**

MiaPaCa2 PDA cells were pretreated with or without T2AA (20  $\mu$ M, 2 h), then exposed or not to T2AA (20  $\mu$ M) +  $\beta$ -lap (2  $\mu$ M) for 2h,  $\pm$  DIC (50  $\mu$ M). Cells also were treated with  $\beta$ -lap (8  $\mu$ M, 2 h). (A) Cells were assessed for DSBs quantified by  $\gamma$ -H2AX (in green) and 53BP1 (in red). Nuclear DNA in cells was also stained using DAPI (in blue). Scale bar = 10  $\mu$ m. (B) Graphical representation of data presented in Fig. 4A. (C) Cells were assessed for total DNA lesions using alkaline comet assays. Comet tail lengths were monitored at 2 h. (D) Graphical representation of data presented in Fig. 4C. Data represent the mean  $\pm$  SD. Student's t tests were performed, \*\*\* $p$  < 0.001, \*\* $p$  < 0.01, \* $p$  < 0.05.

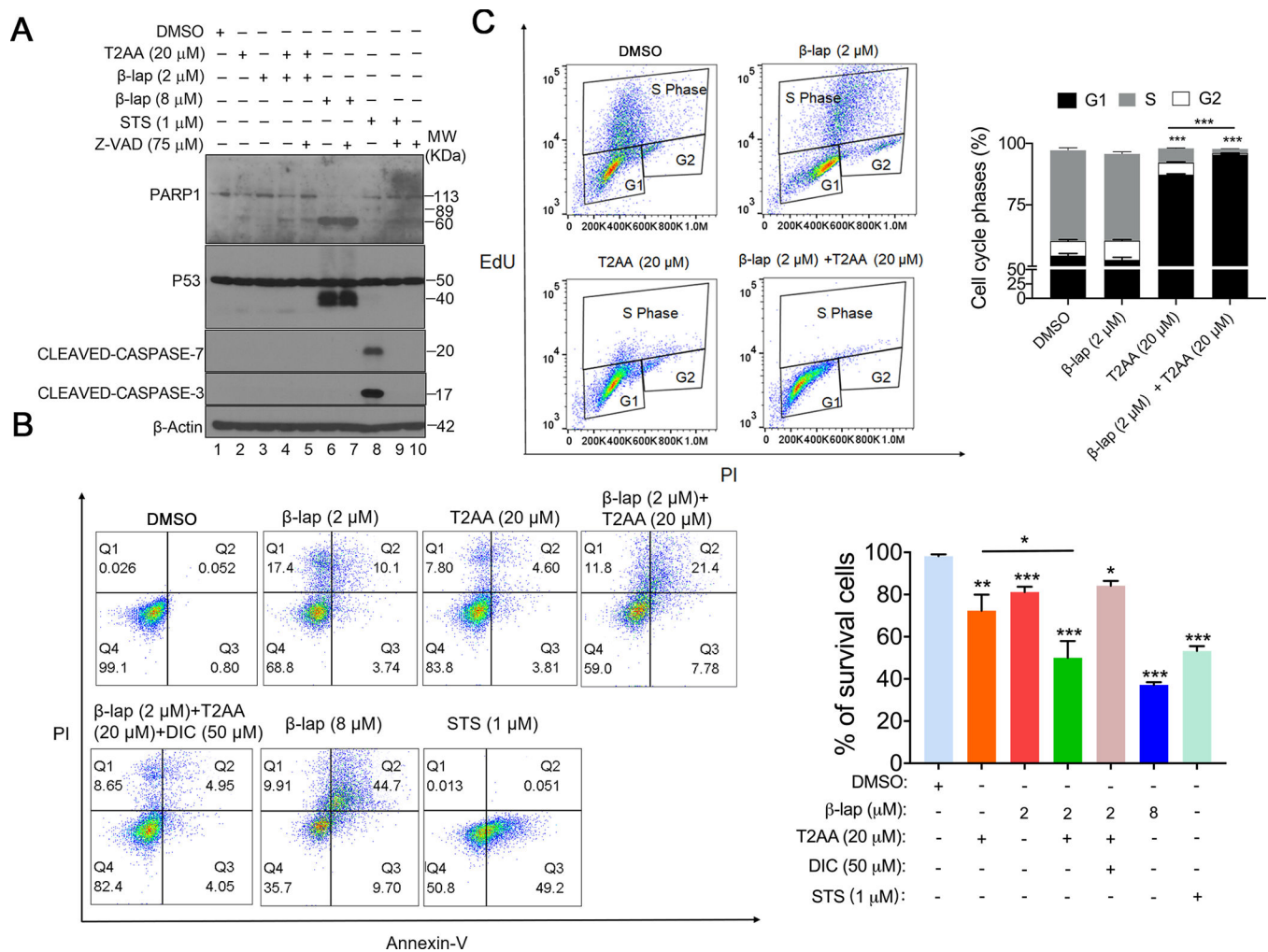


**Fig. 5. T2AA promotes programmed necrosis and G1/S phase cell cycle arrest in  $\beta$ -lapexposed *NQO1*<sup>+</sup> cancer cells**

(A-B) MiaPaCa2 PDA cells were pretreated with or without T2AA (20  $\mu$ M, 2 h) and then treated with or without T2AA (20  $\mu$ M, 2 h) +  $\beta$ -lap (2  $\mu$ M)  $\pm$  DIC (50  $\mu$ M)  $\pm$  ZVAD-fmk (pan-caspase inhibitor, 75  $\mu$ M) for 2 h. Cells were also exposed to staurosporine (STS; 1  $\mu$ M, 18 h) or  $\beta$ -lap (8  $\mu$ M, 2 h)  $\pm$  ZVAD-fmk (75  $\mu$ M, 2 h) to detect apoptotic and programmed necrotic (NAD<sup>+</sup>-Keresis) death pathways. (A) After 36 h, proteolytic markers of cell death, including PARP1 (89 kDa for apoptosis, 60 kDa for programmed necrosis), p53 (40 kDa for programmed necrosis), cleaved caspase-7 (20 kDa for apoptosis), and cleaved caspase-3 (17 kDa for apoptosis), and  $\beta$ -actin (loading control) were assessed. (B) After 36 h, death pathways were assessed and summarized by flow cytometry. Results were separately repeated at least three times in triplicate. (C) Representative images of MiaPaCa2 PDA cells exposed to T2AA (20  $\mu$ M, 4 h) alone,  $\beta$ -lap (2  $\mu$ M, 2 h) alone or a combination of T2AA (20  $\mu$ M, 4 h) +  $\beta$ -lap (2  $\mu$ M, 2 h). Then, the percentages of cells in the G1, S and G2 phases of the cell cycle measured by EdU and PI staining were summarized by flow cytometry. Results were separately repeated at least three times in triplicate. Results (mean  $\pm$  SD) are from three independent experiments. \*\*\* $p$  < 0.001, \*\* $p$  < 0.01, \* $p$  < 0.05 (t tests).

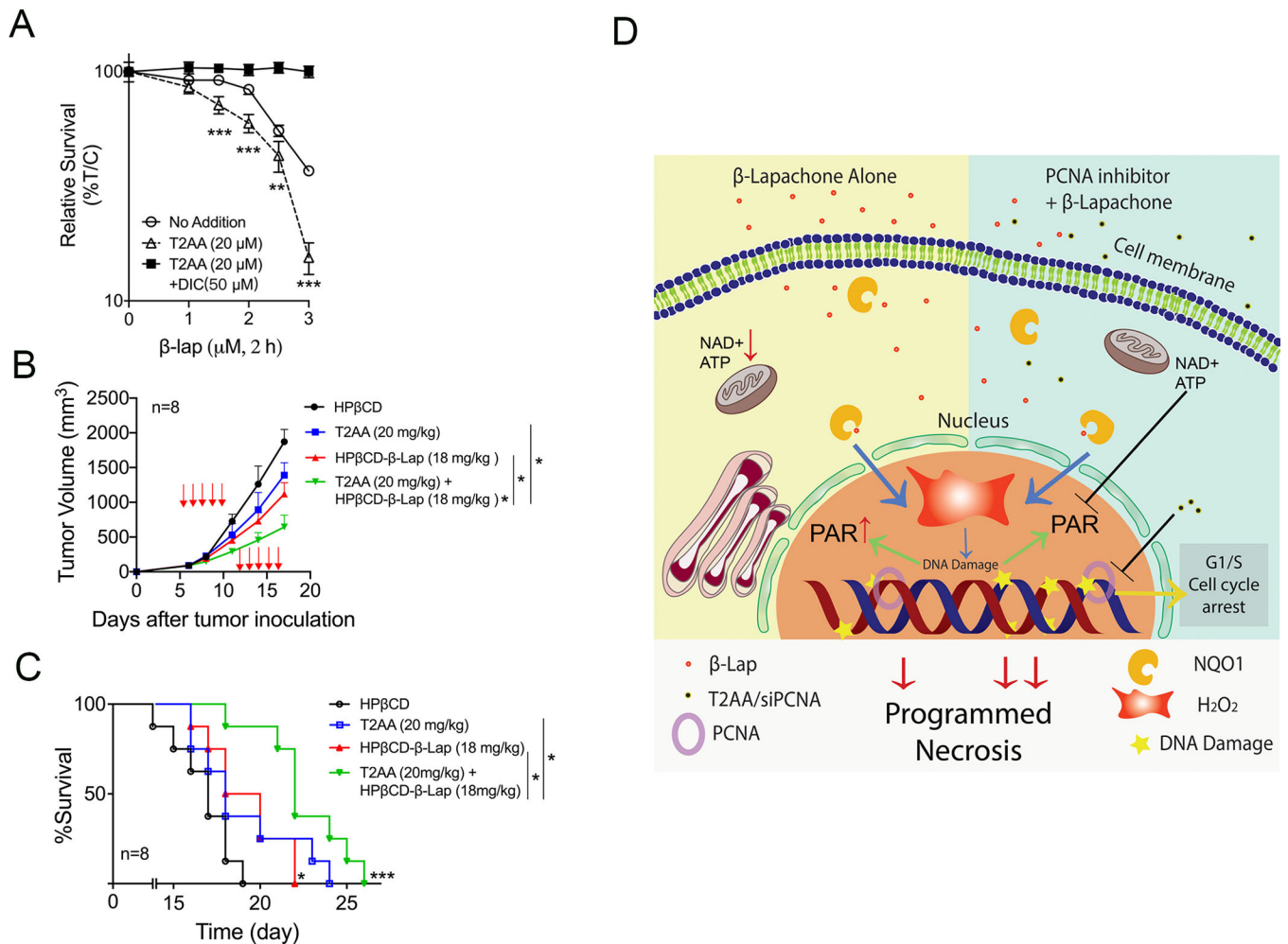


**Fig. 6. T2AA synergizes with β-lapachone against LLC xenografts in C57BL/6 mice**  
**(A)** LLC cells were pretreated with or without T2AA (20 μM, 2 h), then exposed or not to T2AA (20 μM) + β-lap (1–3 μM) for 2h, ± DIC (50 μM). Drugs were removed and cell viability was determined by relative survival assay (DNA assay) 7 days later. All error bars represent the mean ± SD. \*\*\* $p < 0.001$ , \*\* $p < 0.01$ , \* $p < 0.05$  (t tests). **(B, C)** LLC xenografts were established in female C57BL/6 mice weighing ~20 g by subcutaneous injecting  $\sim 2 \times 10^6$  cells. After tumor volumes of  $\sim 50$ – $80$  cm<sup>3</sup> were achieved, mice were randomly divided into four different groups (n=8/group) and treated with HPβCD alone, T2AA (20 mg/kg, i.t.), β-lap (18 mg/kg, i.t.) or T2AA (20 mg/kg, i.t.) 1 h prior to β-lap (18 mg/kg, i.t.). Treatments were given once per day for five consecutive days then recovered 2 days, followed by another five daily injections (red arrows represent treated days). Tumor volume **(B)** and overall survival **(C)** were monitored. Tumor volumes were measured during the 20 days. \*\*\* $p < 0.001$  and \* $p < 0.05$  (t tests). β-Lap (18 mg/kg, i.t.) or combined treatment vs vehicle (HPβCD alone) treatment was determined by log-rank test, \*\*\* $p < 0.001$  and \* $p < 0.05$ . Synergy values were reported based on comparative p values indicated. **(D)** Schematics for a summary of β-lap monotherapy or combination therapy of β-lap with PCNA inhibition.